Assess Flooding Impacts in Urban Environment: Integrating Fluid-Dynamic Simulations in Smart City Digital Twin

Enrico Collini[1], Marco Fanfani[1(✉)], Federico Galli[1], Paolo Nesi[1], and Paola Zamperlin[2]

[1] DISIT Lab, DINFO, University of Florence, Florence, Italy
{enrico.collini,marco.fanfani,federico.galli,
paolo.nesi}@unifi.it
[2] SAGAS, University of Florence, Florence, Italy
paola.zamperlin@unifi.it

Abstract. In recent years, climate change has led to a significant increase in the frequency and intensity of extreme weather events. Among them, floodings represent one of the most critical and dramatic events that can produce casualties and huge damage in urban environments. Therefore, the development of effective tools for the prevention and management of hydrological risks is of paramount importance. In this context, the simulation of flood scenarios and their visualization represent fundamental support tools for decision makers and urban planners to assess risks and identify countermeasures. For these reasons, in this paper, a fluid-dynamic simulation engine integrated into the Snap4City Digital Twin platform is proposed, and, to allow users to observe the results, simulation outputs are encoded as an animated heatmap and visualized on interactive 3D dashboards. Experimental studies comparing the simulation results with the measurements of the 1966 historical flood of Florence, Italy, confirm the validity of the proposed approach.

Keywords: Flooding · Hydrological Risks · Smart City · Digital Twin · Fluid-dynamic Simulation · 3D Dashboard

1 Introduction

The increasing frequency of extreme events resulting from climate change [1], coupled with the expansion of built-up areas connected with urban and population growth, including the spread of residential and economic buildings, as well as mobility or critical infrastructure, requires greater attention to flood-risk mitigation for potentially exposed populations and assets. A city seeking to become resilient must equip itself with tools capable of reducing vulnerability and strengthening its capacity for rapid response. Such resilience can be fostered through a systemic approach to vulnerability assessment, intelligent hydrodynamic monitoring, the prediction of impacts under changing conditions, and the development of appropriate risk-management response systems [2, 3].

© The Author(s), under exclusive license to Springer Nature Switzerland AG 2027
O. Gervasi et al. (Eds.): ICCSA 2026 Workshops, LNCS 16764, pp. 435–449, 2027.
https://doi.org/10.1007/978-3-032-30533-6_29

Over the past two decades, there has been a marked increase in studies devoted to developing models for flood-impact assessment. This trend reflects the growing interest of the scientific community in producing increasingly reliable predictive tools, further enhanced by the availability of data for the accurate reconstruction of digital surface models and by real-time information on meteorological conditions, environmental variables, and contextual factors [4–7].

In this context, Smart City Digital Twins (SCDTs) [8] have emerged as fundamental technologies to support decision makers in facing emergencies and planning solutions to increase urban resilience by integrating multiple urban data sources (including hydrological, transportation, geographic, and infrastructure-related information) with advanced simulation and predictive data analytics to evaluate the effect of possible scenarios. Current experience shows that the adoption of SCDT solutions enhances the accuracy of flood-risk assessment and provides a solid basis for capital allocation, insurability evaluation, and adaptation planning, while also highlighting significant governance, legal, and behavioral constraints. Overall, this approach supports the objectives of the EU Floods Directive[1] by improving risk mapping, preparedness, and the protection of vulnerable populations.

Nevertheless, the exploitation of SCDT in evaluating the impact of floodings is hindered by limited existing hydrodynamic models able to represent flood processes in the built environment, thereby underscoring the need for more comprehensive risk mapping that accounts for multiple flood drivers and their associated impacts [9]. By contrast, simulations based on fluid dynamic models have proved to be considerably more robust, as they are based on physical support for a comprehensive representation of flood processes. However, such simulators are usually not integrated into the SCDT platform.

For these reasons, in this paper, a flooding simulation framework integrated into the Snap4City SCDT platform is proposed. By exploiting physically based models, the simulator can provide accurate reconstructions of flooding events that are visualized on 3D web-based dashboards to allow decision makers to obtain a clear and immediate understanding of the risks and identify critical areas in order to plan adequate responses. The paper is structured as follows: In Sect. 2, the fluid-dynamic simulation engine is presented. Then, in Sect. 3**,** details on ingestion and visualization of simulation results are provided, while in Sect. 4**,** an experimental validation of the simulation results is reported. Finally, conclusions are drawn in Sect. 5.

2 Fluid-Dynamic Simulation Engine

The selection of an appropriate engine to carry out hydrodynamic simulations into the digital twin is a critical step in developing a reliable support decision system to assess flooding risk in an urban environment. In the context of Smart Cities, a simulation tool must not only provide high physical accuracy but also guarantee computational efficiency and seamless integration into automated data pipelines. In addition, preference should be given to open-source solutions to avoid technological lock-in and allow easier and wider distribution.

[1] https://environment.ec.europa.eu/topics/water/floods_en

Among the available open-source solutions, HEC-RAS [10] (Hydrologic Engineering Center's River Analysis System) and LISFLOOD-FP [11] emerged as the most prominent 2D hydrodynamic models in the scientific community. While both models are highly capable of simulating complex fluvial dynamics, LISFLOOD-FP has been preferred following the findings of the comparative study presented in [12], in which it is indicated that LISFLOOD-FP tends to produce superior results in flat urban topographies. Additionally, LISTFLOOD-FP supports native builds for UNIX/Linux open-source operating systems as well as operating natively with standard ASCII Raster formats, facilitating its integration with GIS software (e.g., QGIS [13]) for data pre-processing.

LISFLOOD-FP is a hydrodynamic simulation software developed by the University of Sheffield. It is widely used in scientific literature for simulating fluvial and urban flood propagation due to its optimal balance between computational efficiency and result accuracy. The software is specifically designed to operate on regular raster grids (from 1x1m to 100x100m cells), making it highly suitable for high-resolution urban contexts where capturing micro-topographical features is essential. The model solves a simplified version of the 2D shallow water equations (Saint-Venant Equations [14]), which are appropriate for flows where the water depth is significantly smaller than the horizontal extent. The continuity equation of the Saint-Venant system is:

$$\frac{\partial h}{\partial t} + \frac{\partial (hu)}{\partial x} + \frac{\partial (hv)}{\partial y} = r - f \tag{1}$$

where: h is the water depth, u, v the components of the mean velocity on x and y direction respectively, r the possible rain, and f the infiltration (both expressed in mm/h). This equation describes how the water depth varies in time.

For solving (1), LISFLOOD-FP implements two primary numerical schemes: the Kinematic Wave Approximation and the Local Inertial Formulation, hereafter briefly introduced for completeness.

2.1 Kinematic Wave Approximation

The Kinematic Wave Approximation is a simple approach for water flow rate approximation based on the Manning formula [15]:

$$V = \frac{1}{n} R^{\frac{2}{3}} S^{\frac{1}{2}} \tag{2}$$

where: V is the mean flow velocity in the channel, assuming a constant velocity, $R = A/P$ is the hydraulic radius (in which A is the wetted cross-sectional area of the flow and P the wetted perimeter length of channel boundary in contact with water), $S = \left[-\frac{\delta(h+z)}{\delta x}, -\frac{\delta(h+z)}{\delta y} \right]$ is the channel slope, with z the terrain elevation, and n is the Manning's roughness coefficient.

Given a wide floodplain, in which the width of the plain is much greater than the water depth, the hydraulic radius simplifies to $R \approx h$, and the momentum equation describing

the flow rate $q = hV$ is

$$\begin{cases} q_x = \frac{1}{n} h^{\frac{5}{3}} S_x^{\frac{1}{2}} \\ q_y = \frac{1}{n} h^{\frac{5}{3}} S_y^{\frac{1}{2}} \end{cases} \tag{3}$$

where: q_x, q_y are the flow rate in x and y directions. Finally, the continuity equation can be expressed as:

$$\frac{\partial h}{\partial t} + \frac{\partial q_x}{\partial x} + \frac{\partial q_y}{\partial y} = r - f \tag{4}$$

In summary, the Kinematic Wave model assumes that flow is controlled only by hydraulic slope and resistance to motion, eliminating acceleration terms. Even if this simplification makes the model numerically stable and computationally efficient, it fails to capture accurate water body motions.

2.2 Local Inertial Formulation

The Local Inertial Formulation [16, 17] is an advanced scheme that pairs the continuity Eq. (4) with updated motion equations in which local inertia terms are considered. The motion equations are defined as follows:

$$\begin{cases} \frac{\partial q_x}{\partial t} + gh\frac{\partial H}{\partial x} + g\frac{n^2 q_x |q_x|}{h^{\frac{7}{3}}} = 0 \\ \frac{\partial q_y}{\partial t} + gh\frac{\partial H}{\partial y} + g\frac{n^2 q_y |q_y|}{h^{\frac{7}{3}}} = 0 \end{cases} \tag{5}$$

where g is gravity acceleration, $H = h + z$ is the water surface elevation (h water depth and z ground elevation), and the other terms follow the previous definitions. This formulation is not presented in terms of water flow values but in terms of dynamics. It considers that the dynamic mass of the water needs time to accelerate due to gravity (g) or slope ($\partial H/\partial x$) and it is contrasted by the friction (related to the Manning's coefficient n). This differs from the previous scheme in which acceleration happened instantly without considering the resistance of the mass of the water.

Therefore, this formulation provides a superior balance of physical accuracy and numerical stability, particularly for high-resolution urban simulations. Moreover, it enables the processing of local topography, allowing the simulation to take into account building heights, which are typically integrated by locally increasing the terrain elevation. At high resolutions, the model effectively captures the channeling effect of streets, accumulation in depressed areas, and the barrier effect of buildings.

Indeed, Local Inertia Formulation represents a significant advancement over previous methods, and for this reason, it has been selected as the numerical scheme to be used in the presented solution.

Finally, it is worth remembering that to numerically solve the partial differential equation, it is required to discretize the domain in a grid of cells (also known as a mesh).

2.3 Required Input Data and Produced Outputs

To execute a simulation, LISFLOOD-FP requires several configuration and geographic data files. Terrain elevation is provided in ASCII format (*.asc*), a widely adopted standard in GIS environments that can be used to encode matrices or grids. Each cell in the grid stores elevation data, enabling a discrete yet accurate representation of urban topography. In addition, LISTFLOOD-FP requires a parametrization of the surface roughness (representing the Manning's coefficient) to appropriately model the flow propagation velocity. Such data can be produced in the ASCII format too.

To constrain the resolution of the fluid-dynamic equations, boundary conditions are required. In LISFLOOD-FP, such constraints are specified using the *.bci* and *.bdy* files. The former acts as an index that specifies the domain cells in which the boundary conditions are enforced: in the case of fixed conditions (not changing during the whole simulation), their value is directly set in the *.bci* file. On the other hand, for time varying conditions in the *.bci* file, a pointer to a *.bdy* file that describes the evolution of the constraint during the simulation timespan is put. In particular, the simulation must know from where the flow enters (inlet) and exits (outlet) from the domain. In the inlet cells, the variable flow and water level are specified. Since the domain is considered closed by default, water cannot flow out of the domain without specifying outlet points. Note, however, that by using a sufficiently wide domain with respect to the water body, most cells at the border are never reached by the water. It is instead mandatory to specify the natural outlet of the water body (e.g., the cell covering the position from which the river exits the domain), and in this case, it is also possible to set a free-flow condition to allow water to flow out freely without imposing specific constraints on water levels or discharge.

Initial conditions, used to set the system state at $t = 0$, are specified in the startfile (*.asc*) in which initial water levels for each cell of the domain may be defined. However, it has been noted that improved numerical stability and better simulation results can be achieved by setting the water level at zero in any cell (including the cells covering water bodies) and then allowing the simulator to fill the domain according to the terrain elevation until the water reach a value equal to a reference level (e.g. the average water level of the water bodies in the domain).

To integrate building and other obstacle information, LISFLOOD-FP supports two main approaches for integrating such structures. Topographic modification can be performed locally by (i) increasing terrain elevation in cells corresponding to buildings, simulating them as physical obstacles, or (ii) via roughness modification, increasing local Manning's coefficients to reflect the presence of structures.

All the defined inputs together with additional parameters such as simulation time, sampling time, numerical solver to be used, the Courant–Friedrichs–Lewy (CFL) coefficient to control the numerical stability, etc., are collected in a *.par* file passed to LISFLOOD-FP to run the simulation.

In output, the simulation engine produces a series of temporal raster images in the *.wd* format, one for each time step. Each raster describes system status at a time instant in the form of a matrix, representing the grid used to define the domain, with values indicating the water height (in meters) to be added to the initial terrain elevation provided as input.

3 Flooding Heatmap Generation, Ingestion, and Visualization

To allow the dynamic visualization of the simulation output in an interactive dashboard of the Snap4City platform, further processing and data ingestion pipelines must be executed. Indeed, Snap4City [18] offers 3D interfaces for the visualizations of urban digital twin representation, integrating a number of real-time and historical data, including terrain elevation and 3D models of buildings and city structures [19]. Furthermore, Snap4City provides a heatmap management system: with adequate processing, flooding simulation outputs can be represented as heatmaps (describing the time-varying water level) and used for the visualization of simulation results.

The main workflow used to ingest the outputs of LISFLOOD-FP and enable their visualization into a 3D Snap4City Digital Twin dashboard is presented in Fig. 1. The water level files obtained from the simulation pass through post-processing to transform the data into suitable files to be ingested in the Heatmap Manager system. Once the time-varying heatmaps related to the flooding are ingested into the platform (with metadata and colormap information), the system generates GeoTIFF images that are served via GeoServer to the Snap4City dashboard, allowing users to interact and inspect flooding results through a web-based interface.

3.1 Heatmap Post-processing and Ingestion

The water level data produced by the simulation engine is not directly suitable for integration into a web-based visualization and interaction system due to its large file size. In particular, the simulator generates huge ASCII files that can reach hundreds of megabytes and would result in high latency during data transfer over the web. To address this limitation, the outputs are converted into GeoTIFF by the Heatmap Manager. In order to accomplish such a task, ASCII data are first converted into binary formats accepted by the Heatmap Manager for data ingestion.

The encoding workflow begins with the parsing of *.wd* files describing the water height, from which both header information and depth matrices are extracted. During this phase, cells with depth values below a minimum threshold of 0.01 m are discarded, as they are considered negligible and would unnecessarily increase the final file size. Subsequently, the spatial reference of the data is transformed into UTM Zones, a

coordinate reference system (CRS) suitable for compatibility and widely used as a web mapping standard. Finally, the processed data is serialized into a lightweight binary format (*.con*). In this representation, each record consists of two 32-bit integer coordinates (since UTM coordinates can be represented with integer values) and a single 32-bit floating-point value representing water depth. This structure allows for efficient data transfer and rapid ingestion of huge data. During the processing, each timestamp of the simulation generates a specific instance of the *.con* file as well as related metadata whose details are discussed in the next section.

3.2 Data Ingestion and Publication

The ingestion phase ensures that the encoded heatmaps are properly indexed and made accessible to the platform's visualization tools, enabling their effective use within the digital twin platform.

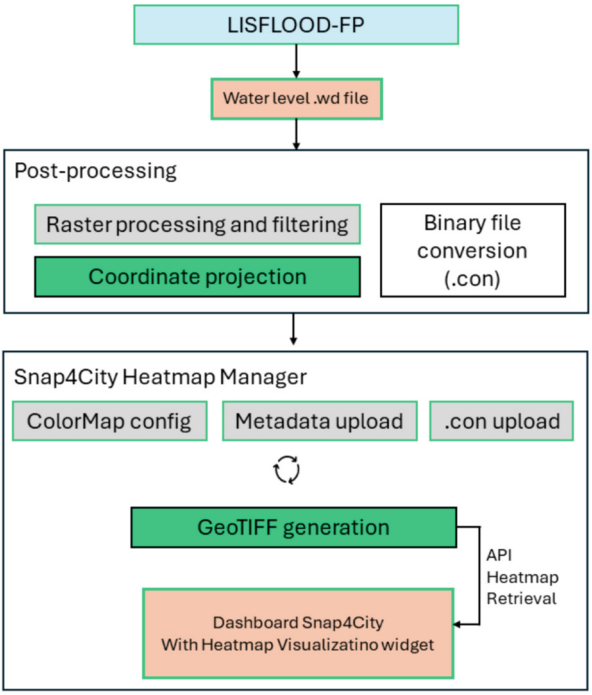

Fig. 1. Workflow flooding simulation data integration in Snap4City platform.

For each simulation timestep, a JSON metadata document is generated and transmitted via REST API to the Snap4City platform. This document contains key attributes required for correct data management and visualization, including the heatmap identifier, cell dimensions, ownership information, and a timestamp formatted according to the ISO 8601 standard. The inclusion of temporal metadata is essential to support time-based navigation and dynamic analysis.

In parallel, a specific color map is associated with the simulation data to convert numerical depth values into an intuitive visual representation. For example, to represent flooding, the color scale can range from dark blue, indicating maximum water depth, to light blue, corresponding to minimum values. This visual encoding enhances interpretability and allows users to quickly identify critical areas affected by flooding.

Once all data and metadata for any simulated time instant have been transmitted to the Heatmap Manager, the manager proceeds to generate GeoTIFF files. Since GeoTIFF is a well-known standard for GIS, this strategy allows the data to be consumed not only within the web-based Digital Twin but also by external spatial tools.

Finally, the created GeoTIFFs (one for each time instant) are sent to the Snap4City GeoServer to enable their distribution in different tile sizes through WMS/WCS protocols, thereby extending accessibility and supporting broader analytical workflows.

3.3 3D MultiDataMap Visualization and Interaction

The final visualization is delivered through a 3D MultiDataMap widget, embedded within a Snap4City dashboard, that provides an immersive representation of the flooding simulation. This environment enables users to explore both spatial and temporal dynamics of flooding in an intuitive and interactive manner.

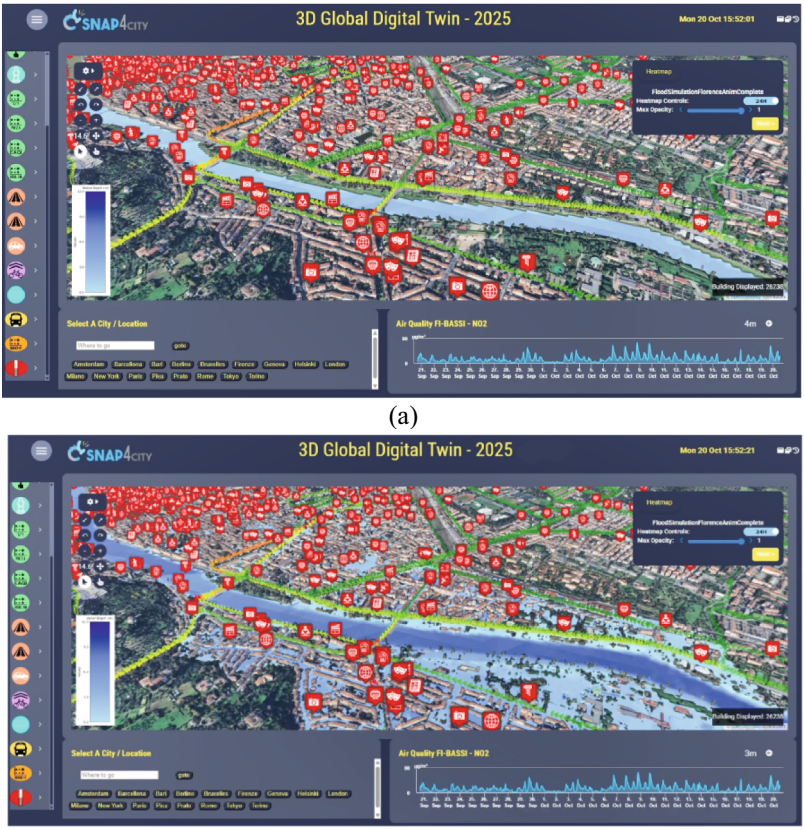

Fig. 2. Snap4City Digital Twin dashboard presenting flooding simulation results. In (a) the initial condition, in (b) an instant in which water overflows into city streets.

A dashboard has been configured in Snap4City using the Dashboard Manager [20] and made accessible via a web browser. The dashboard contains a specific selector that, when clicked, activates the automatic heatmap retrieval, interrogating the GeoServer (via REST APIs) and thus allowing the visualization of the flooding simulation results on the 3D map. A screenshot of the Snap4City Digital Twin dashboard with the flooding heatmap is reported in Fig. 2, in which two different time instants of the simulation are presented. Once the flooding heatmap has been loaded, the simulation results can be inspected thanks to the implemented temporal navigation and animation capability,

which allows users to observe the time-varying evolution of the flood during the simulated period. Controls to change the time instant and animate the heatmap are made available to the user with the panel placed in the top right corner of the dashboard (see Fig. 2). This temporal inspection feature allows decision-makers to analyze the progressive increase and subsequent recession of water levels across the urban area, essential for understanding the dynamics of the event and identifying critical time windows for intervention.

In addition, the visualization integrates heatmaps with high-resolution 3D building models, enhancing the contextual understanding of flood impacts. By overlaying water depth data onto the three-dimensional urban environment, users can directly compare flood levels with building elevations and assess the vulnerability of ground floors and other critical structures. This spatial correlation significantly improves the reliability of impact assessments.

The system also includes interactive controls that allow users to adjust the opacity and intensity of the heatmaps. These functionalities ensure that flood information can be effectively visualized without obscuring other relevant urban data layers. Indeed, several smart city entities are represented in the Snap4City platform and made available to users via the digital twin dashboard: position of point of interest, IoT sensors, road infrastructures, public services, etc. As a result, multiple sources of information can be analyzed simultaneously within a unified and interactive interface. This immersive 3D rendering, capable of visualizing complex flood simulation data intuitively and immediately, together with a plethora of other smart city entities, offers an operational decision-support system enabling the evaluation of urban resilience and plan emergency responses with high spatial and temporal precision.

4 Experimental Validation

In order to quantitatively evaluate the performance of the simulator, experiments have been carried out by comparing the results obtained with measurements taken from real flood events. In this context, data from the historic flood of Florence, Italy, happened in 1966, has been considered.

To run the simulation, a Digital Terrain Model (DTM) of the urban area has been used to model the terrain elevation and identify the bed of the Arno River. The DTM was obtained from Lidar scans in 2011. The render of the DTM is reported in Fig 3. On the other hand, buildings have been modelled into the simulation, exploiting the 3D models available on the Snap4City platform, from which building plants and heights have been obtained. To include buildings as physical obstacles, the terrain elevation was increased accordingly, performing the topographic modification required. Note that, following [21], bridges on the river have been removed since, in the domain representation used by LISFLOOD-FP, they would have appeared as barriers blocking the water flow.

To model the surface roughness, i.e., the Manning's coefficient, a spatial differentiation according to land use has been used. More specifically, three classes have been defined as follows: urban surfaces (e.g., asphalt, concrete) with roughness set to 0.025; green areas with a value of 0.05; and water bodies to which a value of 0.04 has been assigned. The visual representation of the chosen coefficients has been reported in Fig. 4, in which buildings are also highlighted.

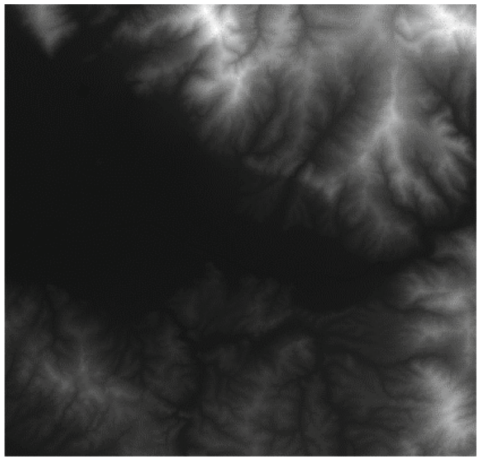

Fig. 3. DTM describing terrain elevation around Florence, Italy.

Regarding the boundary conditions, the inflow flow rate in the inlet has been set according to Arno's discharge measured during the flooding (from late hours of November third to the half day of November fifth, 1966). A plot of the used flow rate is presented in Fig. 5, expressed and m^3/s. Differently, free-flow conditions have been set in the outlet on which a terrain slope of 0.001 has been specified, going outside the simulation domain to allow a graceful outflow. Initial conditions have been defined by setting the water level to zero and then introducing a discharge of 200 m^3/s to allow the simulation to fill the riverbed with water until reaching a threshold level. Such a threshold has been set to 2.5 m, i.e., the average water level of the river, and to reach this value, 1 h and 30 min of simulation time was required.

Finally, the CFL parameter of the simulation has been set to 0.03 to maintain numerical stability during high-volume inflow events. The simulation timespan has been specified at 48 h (from 4:00 PM on November third to 02:00 AM on November 6th) with a sampling time of 20 min, taking into account the time required to reach the average water level in the river as explained above.

To evaluate the balance between simulation precision and computational efficiency, two spatial cell resolutions—1 m^2 and 4 m^2—have been tested.

In order to evaluate the experiment results, ground truth data were obtained from a water depth map of the historical flood event, acquired from the databases of the Arno River Basin Authority [22]. Specifically, the simulation results were analyzed at the peak discharge. The comparison was conducted by evaluating both the areas characterized simply by overestimation or underestimation, as well as the actual error values produced by the simulation. The reference dataset provides an estimate of water elevations in different city areas with a precision of 1 or 2 m, depending on the specific zone (see Fig. 6). Two zones have a 2-m precision describing water depth spanning from 0 to 2 m and from 2 to 4 m. A third zone with 1-m precision describes water depth values from 4 to 5 m.

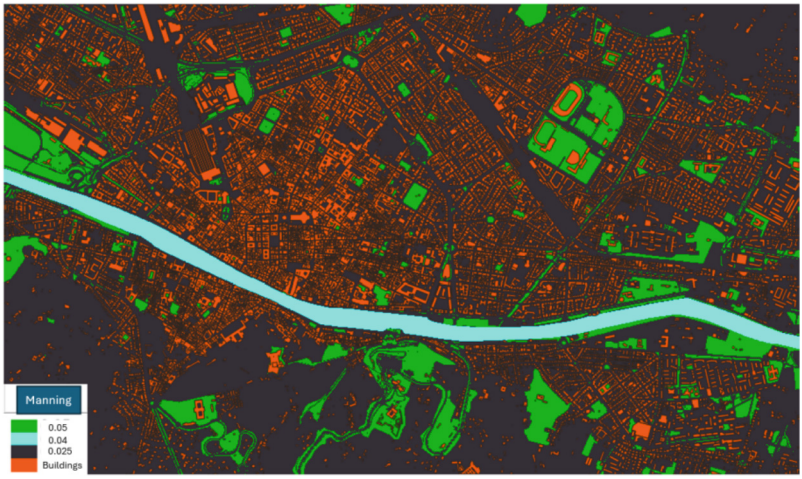

Fig. 4. Map of the surface roughness (Manning's coefficients) in the Florence area. Black areas indicate asphalt and concrete surfaces, green for green areas, cyan for the water body (i.e., the Arno River). In red the buildings of the city.

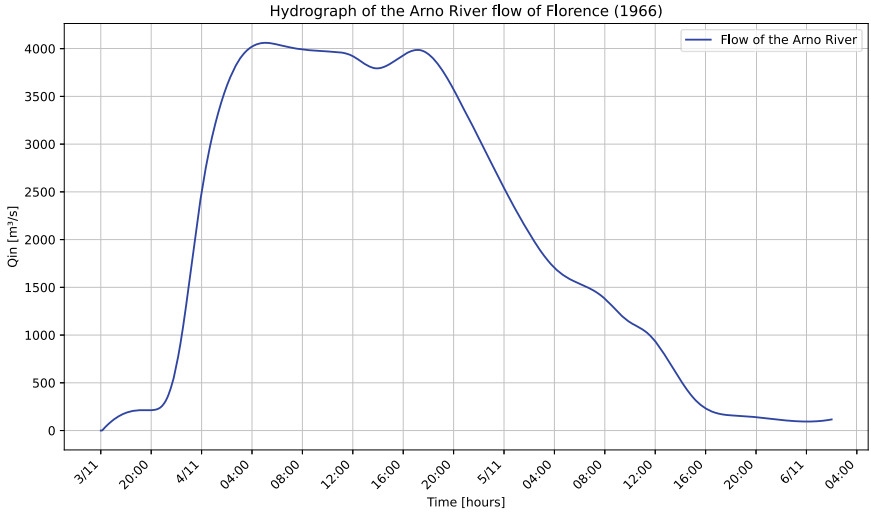

Fig. 5. Historic Arno's discharge measured during the 1966 flooding. From late hours of November 3rd to the afternoon of November 5th, 1966.

The estimated errors are therefore subject to this intrinsic limitation of the reference dataset and have been computed as follows. Depth values from the simulation falling within the precision intervals obtained an error of zero. In the case of overestimation (the simulation outputs higher values w.r.t. the ground truth), the error was calculated relative to the upper limit of the interval. In the case of underestimation, the error was calculated relative to the lower limit of the interval. To evaluate and summarize the errors,

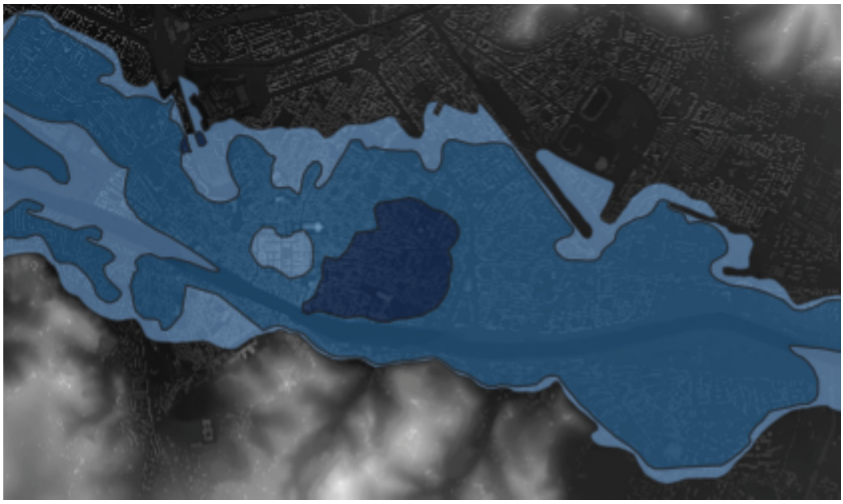

Fig. 6. Flooding reference map for the event of 1966 in Florence, highlighting the three zones: light-blue for water depth values between 0 and 2 meters; mid-blue for values from 2 to 4 meters; dark-blue for values from 4 to 5 meters.

the Mean Average Error (MAE) and the Root Mean Squared Error (RMSE) have been used. The obtained results, reported in Table 1, indicate that increasing the cell size to 4 m^2 does not significantly degrade global accuracy, with MAE varying by only 0.01 m. Differently, with cells of 4 m^2 the domain can be covered with a reduced number of cells (passing from 22.5 M to 5.5 M), and the simulation can be carried out in a shorter time (from 2 weeks to 4 days of computation using a workstation equipped with an 18-core 2.4GHz CPU and 32 GB of RAM). This suggests that, for operational urban flood management, the 4 m^2 resolution provides an optimal compromise between simulation speed and predictive reliability.

Table 1. Experimental results on the simulations performed on 1 m^2 cells and 4 1 m^2 cells.

Parameter	1 m^2 simulation	4 m^2 simulation
Number of cells	22.5 million	5.5 million
Computational time	2 weeks	4 days
MAE	1.11 m	1.10 m
RMSE	1.27 m	1.26 m

In Fig. 7 the absolute error map of the case using 4 m^2 cell size is reported, showing the 6 AM of the fourth of November, the peak of the Arno discharge (see Fig. 5). Most of the errors are due to how buildings are modelled: indeed, 3D models used are solid blocks without apertures (like fences, arcs, door, or windows) in which water usually flow, thus creating impenetrable barriers. In addition, it is important to note that the

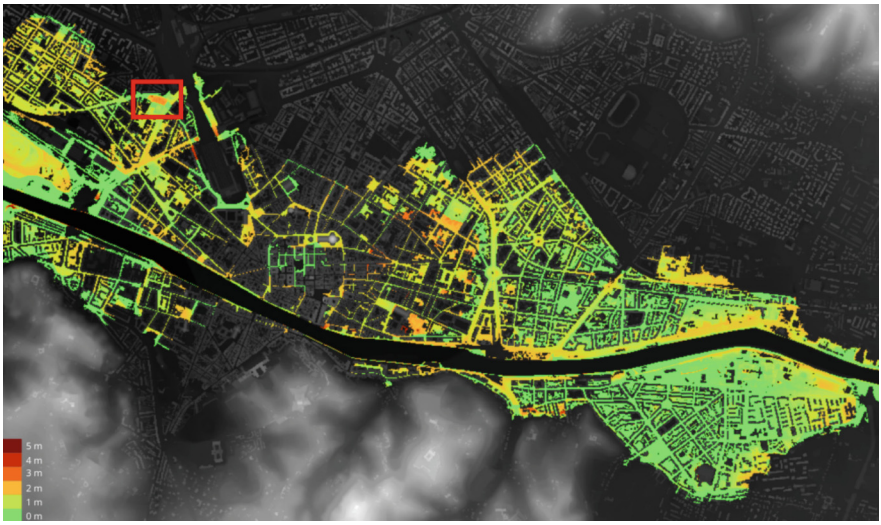

Fig. 7. Flooding absolute error map from the simulations using 4 m^2 cell compared to the data from the 1966 flooding (at 6AM of 4th of November, near the discharge peak). In the red box in the top left corner an area obtaining large errors due to changes in the urban landscape between the 1966 (year of the Florence flooding) and 2011 (year of DTM acquisition).

urban environment changed between 1966 and 2011 (when the DTM was acquired). For example, the large errors obtained in the area highlighted with the red box in Fig. 7 are due to the fact that in the area in 2011, there was a building construction site that created a huge excavation in the ground, while it was a flat area in 1966. Nevertheless, the model effectively captured the complex flood dynamics of a dense urban area such as Florence, with extreme errors occurring only in isolated areas affected by micro-topographical features or stagnation zones.

5 Conclusions

In this paper, a framework for evaluating flooding risks and impacts in urban scenarios has been presented. The solution leverages the LISFLOOD-FP simulation engine, exploiting the Local Inertial Formulation, for solving the fluid-dynamic problem, and it is integrated into the Snap4City Smart City Digital Twin platform that allow a seamless ingestion of the simulation results, that are encoded as series of time-varying heatmaps, and, finally provided to the users via web-based interactive 3D dashboards in which the flooding simulation can be navigated on both space and time axes.

Results obtained by simulating the historical flooding of Florence, which happened from the third to the sixth of November 1966, have demonstrated the reliability of the solution. In addition, tests considering different mesh generation (for the discretization of the domain) using cells of $1m^2$ and $4m^2$ have shown that wider cells provide a significant reduction of computational times without a strong loss in accuracy.

Therefore, the proposed solution realizes a concrete data-driven and simulation-based support decision tool to help decision makers in analyzing flooding dynamics,

identifying critical areas, and, thus, planning emergency responses and countermeasures to improve the smart city resilience.

Acknowledgments. This work has been carried out in the context of the Interreg Euro-MED TOURISMO project "TOURism Innovative and Sustainable Management of flOws", co-funded by the European Union (Euro-MED0200900).

Disclosure of Interests. The authors have no competing interests to declare that are relevant to the content of this article.

References

1. Schreider, S.Y., Smith, D.I., Jakeman, A.J.: Climate change impacts on urban flooding. Clim. Chang. **47**, 91–115 (2000). https://doi.org/10.1023/A:1005621523177
2. de Oliveira, A.K.B., et al.: Evaluating the role of urban drainage flaws in triggering cascading effects on critical infrastructure, affecting urban resilience. Infrastructures **7**(11), 153 (2022). https://doi.org/10.3390/infrastructures7110153
3. Hsu, C.-W., Liu, C.-F., Stearns, L., Brody, S., Mostafavi, A.: Spillover effects of built-environment vulnerability on resilience of businesses in urban crises, 106376. Sustain. Cities Soc. **127** (2025). https://doi.org/10.1016/j.scs.2025.106376
4. Hammond, M.J., Chen, A.S., Djordjević, S., Butler, D., Mark, O.: Urban flood impact assessment: a state-of-the-art review. Urban Water J. **12**(1), 14–29 (2015). https://doi.org/10.1080/1573062X.2013.857421
5. Gao, P., Gao, W., Ke, N.: Assessing the impact of flood inundation dynamics on an urban environment. Nat. Hazards **109**, 1047–1072 (2021). https://doi.org/10.1007/s11069-021-04868-6
6. Zandsalimi, Z., Feizabadi, S., Yazdi, J., et al.: Evaluating the impact of digital elevation models on urban flood modeling: a comprehensive analysis of flood inundation, Hazard mapping, and damage estimation. Water Resour. Manag. **38**, 4243–4268 (2024). https://doi.org/10.1007/s11269-024-03862-4
7. Dong, B., Xia, J., Wang, X.: Comprehensive flood risk assessment in highly developed urban areas, 132391. J. Hydrol. **648** (2025). https://doi.org/10.1016/j.jhydrol.2024.132391
8. Adreani, L., et al.: Digital twin framework for Smart City solutions. In: DMSVIVA 2022 - Proceedings of the 28th International DMS Conference on Visualization and Visual Languages, pp. 1–8 (2022). https://doi.org/10.18293/DMSVIVA22-012
9. Sebastian, A., Juan, A., Bedient, P.B.: Chapter 5 - Urban Flood Modeling: Perspectives, Challenges, and Opportunities, Editor(S): Samuel Brody, pp. 47–60. Baukje Bee Kothuis, Coastal Flood Risk Reduction, Elsevier, Yoonjeong Lee (2022)
10. Brunner, G. W.: HEC-RAS River Analysis System. Hydraulic User's Manual. Version 1.0 (1995)
11. Bates, P., Trigg, M., Neal, J., & Dabrowa, A.: Lisflood-fp. User manual. School of Geographical Sciences, University of Bristol. Bristol, UK (2013)
12. Moghim, S., Gharehtoragh, M.A., Safaie, A.: Performance of the flood models in different topographies. J. Hydrol. **620**, 129446 (2023)
13. QGIS software.: https://qgis.org/ (Accessed on 30th Mar 2026)
14. de Saint-Venant, A.J.C.: Théorie du mouvement non-permanent des eaux, avec application aux crues des rivières et à l'introduction des marées dans leur lit. CR Acad. Sci. Paris. **73**(147–154), 237–240 (1871)

15. Manning, R.: On the flow of water in open channels and pipes. Trans. Inst. Civil Eng. Ireland **20**, 161 (1891)
16. De Almeida, G.A., Bates, P., Freer, J.E., Souvignet, M.: Improving the stability of a simple formulation of the shallow water equations for 2-D flood modeling. Water Resour. Res. **48**(5) (2012)
17. Bates, P.D., Horritt, M.S., Fewtrell, T.J.: A simple inertial formulation of the shallow water equations for efficient two-dimensional flood inundation modelling. J. Hydrol. **387**(1–2), 33–45 (2010)
18. Adreani, L., Bellini, P., Colombo, C., et al.: Implementing integrated digital twin modelling and representation into the Snap4City platform for smart city solutions. Multimed. Tools Appl. **83**, 37121–37146 (2024). https://doi.org/10.1007/s11042-023-16838-0
19. Adreani, L., Colombo, C., Fanfani, M., Nesi, P., Pantaleo, G., Pisanu, R.: A photorealistic 3D city modeling framework for Smart City digital twin. In: 2022 IEEE International Conference on Smart Computing (SMARTCOMP), pp. 299–304, Helsinki, Finland (2022). https://doi.org/10.1109/SMARTCOMP55677.2022.00071
20. Bellini, P., Fanfani, M., Nesi, P., Pantaleo, G.: Snap4City dashboard manager: a tool for creating and distributing complex and interactive dashboards with no or low coding, 101729. SoftwareX. **26** (2024). https://doi.org/10.1016/j.softx.2024.101729
21. Neal, J.C., Bates, P.D., Fewtrell, T.J., Hunter, N.M., Wilson, M.D., Horritt, M.S.: Distributed whole city water level measurements from the Carlisle 2005 urban flood event and comparison with hydraulic model simulations. J. Hydrol. **368**(1–4), 42–55 (2009). https://doi.org/10.1016/j.jhydrol.2009.01.026
22. Arno River Basin Authority: Flood Hazard Map – Discharge, (2015). http://www.adbarno.it/adb/?page_id=5372 (Accessed on 12 Mar 2026)